Spin Reorientation Transition in Single-Domain (Ga, Mn)As

K.-Y. Wang,[1] M. Sawicki,[2,*] K. W. Edmonds,[1] R. P. Campion,[1] S. Maat,[3] C. T. Foxon,[1] B. L. Gallagher,[1] and T. Dietl[2,4]

[1]*School of Physics and Astronomy, University of Nottingham, Nottingham NG7 2RD, United Kingdom*
[2]*Institute of Physics, Polish Academy of Sciences, al. Lotników 32/46, PL-02668 Warszawa, Poland*
[3]*Hitachi Global Storage Technologies, San Jose Research Center, 650 Harry Road, San Jose, California 95120, USA*
[4]*ERATO Semiconductor Spintronics Project, al. Lotników 32/46, PL-02668 Warszawa, Poland and Institute of Theoretical Physics, Warsaw University, PL-00681 Warszawa, Poland*

(Received 8 July 2005; published 16 November 2005)

We demonstrate that the interplay of in-plane biaxial and uniaxial anisotropy fields in (Ga, Mn)As results in a spin reorientation transition and an anisotropic ac susceptibility which is fully consistent with a simple single-domain model. The uniaxial and biaxial anisotropy constants vary, respectively, as the square and fourth power of the spontaneous magnetization across the whole temperature range up to T_C. The weakening of the anisotropy at the transition may be of technological importance for applications involving thermally assisted magnetization switching.

DOI: 10.1103/PhysRevLett.95.217204 PACS numbers: 75.50.Pp, 75.30.Gw, 75.70.−i

Following the emergence of the ferromagnetic semiconductor (Ga, Mn)As as a test bed for semiconductor spintronics, intensive efforts have been dedicated to its material development [1]. In early studies [2] it was concluded that (Ga, Mn)As suffered from very high compensation, and a large magnetization deficit leading to concern that there were fundamental problems with this, and by implication other, dilute ferromagnetic semiconductors. However, it has now been established that the observed nonideal behavior arose from extrinsic defects [3]. Studies of carefully prepared samples have now shown that compensation can be very low [4] and the magnetic moment per Mn can attain close to its free ion value [5]. It is now generally accepted that (Ga, Mn)As is a well-behaved mean field ferromagnet with a Curie temperature T_C that increases linearly with substitutional Mn concentration [6]. Furthermore, (Ga, Mn)As films generally show excellent micromagnetic properties that can be described both phenomenologically and on the basis of microscopic theories [7,8].

However, some uncertainties remain about the intrinsic sample homogeneity, and to what extent this may influence the magnetic properties. It has been suggested that microscopic phase segregation may be energetically favorable leading to clustering of Mn atoms [9,10]. Very recently it has been argued that dc and ac magnetometry results indicate segregation into two distinct ferromagnetic phases [11]. In this Letter we establish a unified description of the dc and ac magnetic properties of (Ga, Mn)As and show that features interpreted as evidence for mixed phases in fact arise from a single-domain spin reorientation transition (SRT) which further establishes the excellent micromagnetic properties of this system, and which may have technological applications.

It is generally accepted that the ferromagnetic Mn-Mn interaction in (Ga, Mn)As is mediated by band holes, whose Kohn-Luttinger amplitudes are primarily built up of As $4p$ orbitals [2]. Since in semiconductors the Fermi energy is usually smaller than the spin-orbit energy, the confinement or strain-induced anisotropy of the valence band can lead to sizeable anisotropy of spin properties. (Ga, Mn)As grown on GaAs(001) is under compressive strain, which for high or low compensation leads to magnetic easy axes along the growth [001] or in-plane directions, respectively. Quantitative calculations within the mean field p-d Zener model give the full account for the observed easy [001] axis $\Leftrightarrow$ easy plane SRT [12]. Very recently, it has been realized that another in-plane [110] $\Leftrightarrow$ [1$\bar{1}$0] SRT may take place due to the presence of an in-plane uniaxial anisotropy [12–17]. The [110] and [1$\bar{1}$0] orientations are equivalent in the bulk and the microscopic origin remains unclear; however, the observed behavior is consistent with the mean field p-d Zener model if an additional symmetry-breaking strain is introduced [17]. There is much interest in developing new approaches to magnetization switching in nonvolatile logic operations [18–20], which calls for precise control of magnetic anisotropy (required weak for manipulation and strong for storage). In this context, both the existence of SRTs and the understanding of their origins is of a topical interest since it can directly lead to new magnetization manipulation schemes for future spintronics. In this Letter, a new [100] $\Leftrightarrow$ [1$\bar{1}$0] spin reorientation mechanism, related to self-cancellation of two major biaxial and uniaxial in-plane contributions to the magnetic anisotropy, is evidenced and fully accounted for.

Phenomenologically, the magnetic energy of an isolated in-plane magnetic domain can be described as:

$$E = -K_C \sin^2(2\theta)/4 + K_U \sin^2\theta - MH\cos(\varphi - \theta), \quad (1)$$

where K_C and K_U are the lowest order biaxial and uniaxial anisotropy constants, H is the external field, M the magnetization, and θ and φ are the angle of M and H to the [1$\bar{1}$0] direction. This simple model describes experimental ferromagnetic resonance [16], magnetotransport [14], and

magneto-optical [15] data remarkably well, indicating that, at least away from the reversal fields, macroscopically large (Ga, Mn)As films tend to align in a single-domain state. However, the biaxial and uniaxial terms may each have a different dependence on the magnetization, so that a complicated temperature dependence of the magnetic anisotropy is expected [21]. In particular, at a temperature where $K_U = K_C$, the system should undergo a 2nd order magnetic SRT from the biaxial-dominated case when $K_U < K_C$, to a uniaxial realm when $K_U > K_C$. In this Letter we extract the temperature dependence of K_U and K_C for a (Ga, Mn)As film using Eq. (1), and show that the observed transition of the in-plane anisotropy from biaxial to uniaxial is consistent with these values. Furthermore, we show that the transition gives rise to a peak in the temperature dependence of the ac susceptibility well below T_C, even for a well-behaved single-phase sample, due to cancellation of anisotropy contributions. This can be distinguished from a ferromagnetic-to-paramagnetic transition by its dependence on the applied magnetic field direction.

A series of 50 nm (Ga, Mn)As epilayers was grown by molecular beam epitaxy using As_2. Full details of the growth are given elsewhere [22]. The Mn concentration x is determined by x-ray diffraction and secondary ion mass spectrometry. We focus on results for a sample with $x = 0.022$, but qualitatively similar magnetic properties are observed for as-grown samples with $x = 0.056$ and $x = 0.09$. The hole concentration for this sample, determined by low-temperature high-field Hall effect measurements, is 3.5×10^{20} cm^{-3}. SQUID magnetometry is used to determine the projected magnetization and ac susceptibility along the measurement axis, which is parallel to the applied magnetic field.

Figure 1 shows the measured projections of the remnant magnetization along the [110], [1$\bar{1}$0], and [100] directions, $M_{[110]}$, $M_{[1\bar{1}0]}$, and $M_{[100]}$, for increasing temperature, recorded after cooling the sample through T_C under a 1000 Oe field. The trapped field in the magnet during these measurements is around 0.1 Oe. At low temperatures, the easy axes are close to the in-plane [100] and [010] orientations, while the uniaxial anisotropy favoring the [1$\bar{1}$0] orientation emerges with increasing temperature. Above around 30 K the remnant magnetization is fully aligned with the [1$\bar{1}$0] direction: $M_{[100]}$ is smaller than $M_{[1\bar{1}0]}$ by cos(45°), while $M_{[110]}$ is close to zero. If the sample is in a single-domain state throughout these measurements, then $M_{[100]}$ should be given by $M_S \cos(45° - \theta)$, where $\theta = \arctan(M_{[110]}/M_{[1\bar{1}0]})$, and $M_S^2 = M_{[110]}^2 + M_{[1\bar{1}0]}^2$. As shown in Fig. 1, this is in good agreement with the measured $M_{[100]}$ over most of the temperature range with only a small deviation observed in the region close to the transition between biaxial and uniaxial anisotropy, at around 25 K. This compliance with simple geometrical considerations is a strong indication that the system behaves as a single, uniform domain, so that Eq. (1) can be used to extract the anisotropy constants K_U and K_C.

The dependence of $M_{[110]}$, $M_{[1\bar{1}0]}$, and $M_{[100]}$ on external magnetic field can be obtained by minimizing the energy given by Eq. (1) with respect to θ. For the uniaxial easy [1$\bar{1}$0] axis this gives: $H = -2(K_U + K_C)M_{[1\bar{1}0]}/M_S^2 + 4K_C M_{[1\bar{1}0]}^3/M_S^4$ for $K_C > K_U$, or $M_{[1\bar{1}0]} = \mathrm{sgn}(H)M_S$ for $K_C < K_U$; while for the uniaxial hard [110] axis, the expression is $H = 2(K_U - K_C)M_{[110]}/M_S^2 + 4K_C M_{[110]}^3/M_S^4$. The simplest way to obtain K_C and K_U is by fitting the [110] magnetization curve to this expression. Such a fit is shown in the inset to Fig. 2. However, at low temperatures, the curvature of the $M_{[110]}(H)$ becomes small, and so the

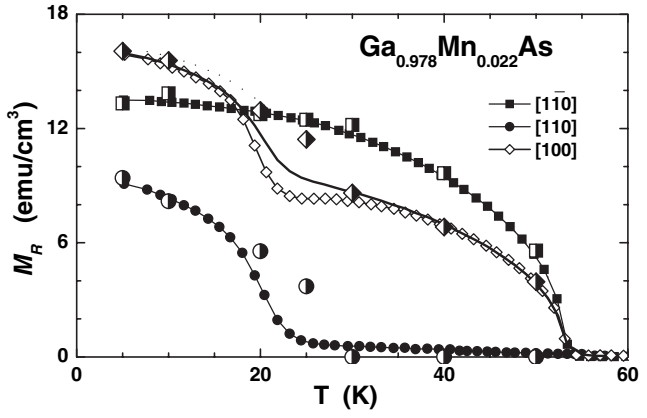

FIG. 1. Remnant magnetization along [1$\bar{1}$0], [110], and [100] axes vs increasing temperature; (line) remnant magnetization along [100] extracted from the [1$\bar{1}$0] and [110] curves assuming single-domain behavior; (corresponding half-filled symbols) remnant magnetization calculated from Eq. (1) using the anisotropy constants obtained from the analysis of $M(H)$ loops measured at selected temperatures.

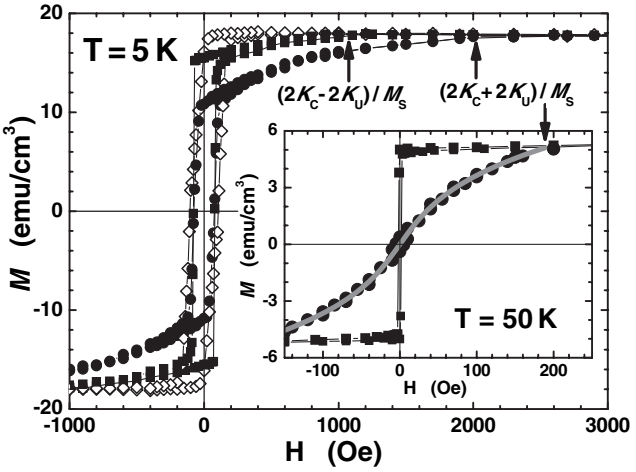

FIG. 2. Symbols as in Fig. 1. $M(H)$ loops along the [1$\bar{1}$0], [110], and [100] axes at 5 K, with the arrows indicating the intersection points which are used to obtain K_U and K_C at low temperature. (inset) $M(H)$ loops along the [1$\bar{1}$0] and [110] axes at 50 K, plus the fit (thick gray line) to the hard axis curve used to obtain K_U and K_C. The arrow indicates the intersection point for uniaxial hard axis measurement.

uncertainties in K_U and K_C become large. In this regime we determine K_C and K_U from the anisotropy fields at which the magnetization is fully rotated in the direction of the external magnetic field, i.e., when the magnetization projections $M_{[110]}$ and $M_{[1\bar{1}0]}$ coincide with M_S, as shown in Fig. 2. The corresponding fields are given by $2(K_C + K_U)/M_S$ and $2(K_C - K_U)/M_S$, respectively. We then confirm that the obtained values are in agreement with the $M_{[110]}(H)$ curve. The values of K_U and K_C for the studied sample are shown in Fig. 3. K_C is larger than K_U at low temperatures, but decreases more rapidly with increasing temperature, so that $K_C \cong K_U$ at around 30 K. Therefore, a transition from biaxial to uniaxial anisotropy is expected around this point, as is observed in Fig. 1. The measured K_U and K_C allow us to obtain the easy axis direction θ at each temperature from Eq. (1), from which we can predict the values of $M_{[110]}$, $M_{[1\bar{1}0]}$, and $M_{[100]}$ at remanence. These are shown by the half-filled symbols in Fig. 1. Apart from a small overestimation of the SRT temperature, which is due to the uncertainty in determining K_U and K_C, this method is found to reproduce the measured remanence versus temperature behavior.

K_C and K_U are plotted versus M_S in the inset of Fig. 3, showing a power-law dependence with $K_C = (0.17 \pm 0.05)M_S^{(3.8\pm0.2)}$ and $K_U = (11 \pm 2)M_S^{(2.1\pm0.1)}$. Thus, the uniaxial and biaxial anisotropy constants show the expected 2nd and 4th order power-law dependence on M_S, respectively [21]. This finding demonstrates that both K_C and K_U depend on *the same* magnetization, and therefore correspond to *the same* magnetic phase. This conclusively rules out a mixed phase concept (exchange coupled or otherwise) [11] as responsible for the uniaxial anisotropy. The single-domain model therefore provides us with the basis for understanding the magnetization rotation in the whole sample, for example, in the response to a weak ac magnetic field.

Measurements of the real and imaginary parts of the ac magnetization, m' and m'', along the [100], [110], and $[1\bar{1}0]$ axes, in response to a 5 Oe, 11 Hz driving field, are shown in Figs. 4(a) and 4(b). Similar to a previous report [11], two peaks are observed along [100], one close to T_C and one close to the SRT. These two peaks were interpreted by Hamaya *et al.* [11] as arising from ferro- to paramagnetic transitions of two phase-segregated distinct magnetic phases, with biaxial and uniaxial magnetic anisotropies, respectively. However, Fig. 4 shows that the low T peak is not present for $[1\bar{1}0]$, while the peak close to T_C is very small for [110]. This strong dependence of the peak amplitudes on the orientation of the driving field argues against the interpretation of Hamaya *et al.* [11], and indicates instead that the peaks result from the interplay of the biaxial and uniaxial contributions to the magnetic anisotropy. When K_C is only slightly larger than K_U, the biaxial easy axes lie close to and on either side of the $[1\bar{1}0]$ direction, and the energy barrier separating them becomes very small. Therefore, a small magnetic field applied away from the $[1\bar{1}0]$ direction produces a relatively large increase of the projected magnetization along the field direction, and thus a large (dc or ac) susceptibility is measured. Meanwhile, the susceptibility along the $[1\bar{1}0]$ direction is much smaller, since a small applied field can only rotate the magnetization by the small angle between the easy axis and the $[1\bar{1}0]$ axis. To confirm this interpretation,

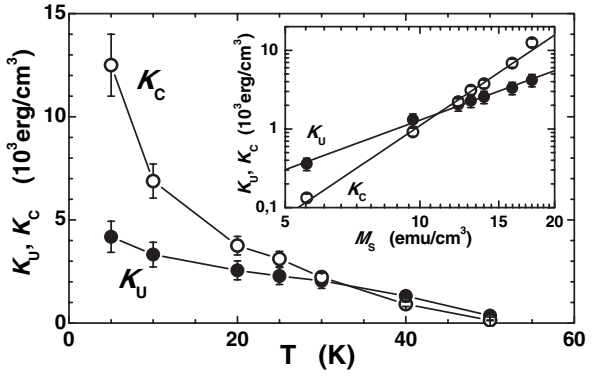

FIG. 3. K_U and K_C, extracted from $M(H)$ loops, vs temperature; (inset) K_U and K_C vs saturation magnetization.

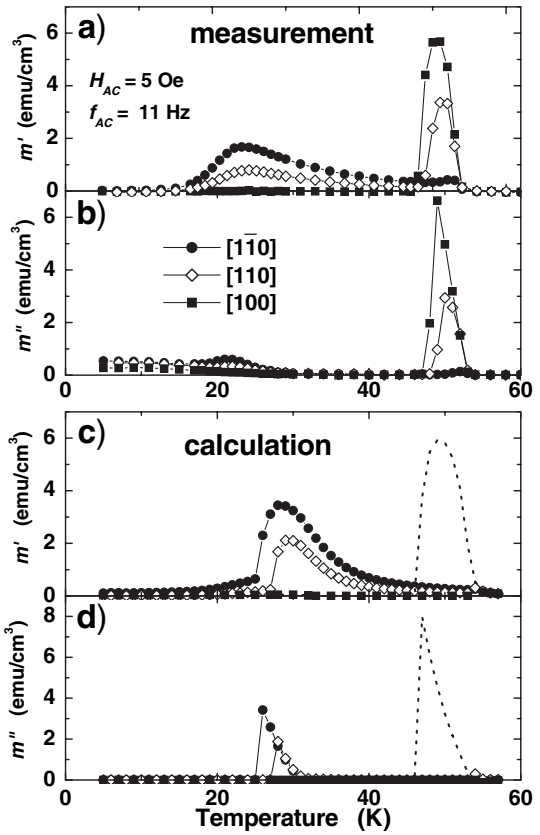

FIG. 4. (a), (b) Real and imaginary parts of the linear ac susceptibility under a 5 Oe, 11 Hz driving field, for measurements along [110], $[1\bar{1}0]$, and [100] axes. (c), (d) Calculated linear ac susceptibility under 5 Oe, using Eq. (1) and the measured dependence of K_C and K_U on M_S (taken from inset to Fig. 3).

we perform a numerical simulation of the ac susceptibility measurement, calculating the signals $m' \sin(\omega t)$ and $m'' \cos(\omega t)$ in response to an applied field $H \sin(\omega t)$. The simulated results shown in Figs. 4(c) and 4(d) are obtained from Eq. (1) with no free parameters, using only the measured $M_S(T)$ and the obtained power-law dependencies of K_C and K_U on M_S. Considering the simplicity of the model, the calculation reproduces the position, shape and angle dependence of the peak at the reorientation transition remarkably well.

The peak close to T_C, which is not reproduced by the calculation, is in small part due to the transition of the system to a paramagnetic state, but is predominantly due to the rapid decrease of the coercivity H_C close to T_C. As shown in Fig. 2 (inset), $H_C = 2$ Oe for $[1\bar{1}0]$ at 50 K, so it is significantly lower than the driving field. The field is therefore sufficient to produce a complete reversal of the magnetization. Equation (1) only includes coherent rotation, so it overestimates the reversal field needed, which is why this peak does not appear in the calculated result. Experimentally, we obtain $H_C \simeq (1 - T/T_C)^2 \times 150$ Oe close to T_C for the $[1\bar{1}0]$ direction. If this is explicitly included in the numerical simulation, by forcing a 180° rotation of the magnetization if the driving field exceeds this value, then the peak close to T_C is reproduced [dashed lines in Figs. 4(c) and 4(d)]. Finally, the coercivity of (Ga, Mn)As is known to be frequency dependent [13], resulting in the frequency dependence of the ac susceptibility near T_C reported in Ref. [11].

The susceptibility peak at the reorientation transition occurs because the field required to rotate the magnetization between the biaxial easy axes becomes very small at this point. However, the energy barrier opposing a 180° reversal remains large. Therefore, a 90° rotation of the low-temperature magnetization could be achieved by heating to the reorientation temperature, followed by cooling in a weak external field. This may be important for thermally assisted writing schemes, in which a laser pulse is used to assist the magnetization reversal of a high anisotropy material, as the temperature where softening of the anisotropy occurs (and thus the laser fluence needed) may be substantially reduced by the presence of a reorientation transition. Such schemes involving 90° rotation have been explored only recently [20]. Since a similar combination of uniaxial plus biaxial anisotropy may be observed in systems showing room temperature ferromagnetism, such as Fe/InAs(001) [23], this may be of technological relevance.

In summary, the recently reported ac susceptibility peak at the reorientation transition temperature in (Ga, Mn)As is shown to occur for single-phase, single-domain systems, and is a consequence of the cancellation of uniaxial and biaxial magnetic anisotropy fields. The softening of the anisotropy at the transition may be important for magnetization manipulation in spintronics devices.

Support of EPSRC, EU FENIKS (G5RD-CT-2001-0535), and Polish PBZ/KBN/044/PO3/2001 projects is gratefully acknowledged.

*Electronic address: mikes@ifpan.edu.pl

[1] H. Ohno, J. Magn. Magn. Mater. **272**, 1 (2004).
[2] F. Matsukura, H. Ohno, and T. Dietl, in: *Handbook of Magnetic Materials*, edited by K. H. J. Buschow (Elsevier, New York, 2002), Vol. 14, p. 1.
[3] K. M. Yu *et al.*, Phys. Rev. B **65**, 201303(R) (2002).
[4] K. Y. Wang *et al.*, J. Appl. Phys. **95**, 6512 (2004).
[5] K. W. Edmonds *et al.*, Phys. Rev. B **71**, 064418 (2005).
[6] T. Jungwirth *et al.*, Phys. Rev. B **72**, 165204 (2005).
[7] T. Dietl, H. Ohno, and F. Matsukura, Phys. Rev. B **63**, 195205 (2001).
[8] M. Abolfath, T. Jungwirth, J. Brum, and A. H. MacDonald, Phys. Rev. B **63**, 054418 (2001).
[9] M. van Schilfgaarde and O. N. Mryasov, Phys. Rev. B **63**, 233205 (2001).
[10] H. Raebiger, A. Ayuela, and J. von Boehm, Phys. Rev. B **72**, 014465 (2005).
[11] K. Hamaya, T. Taniyama, Y. Kitamoto, T. Fujii, and Y. Yamazaki, Phys. Rev. Lett. **94**, 147203 (2005).
[12] M. Sawicki *et al.*, Phys. Rev. B **70**, 245325 (2004).
[13] D. Hrabovsky *et al.*, Appl. Phys. Lett. **81**, 2806 (2002).
[14] H. X. Tang, R. K. Kawakami, D. D. Awschalom, and M. L. Roukes, Phys. Rev. Lett. **90**, 107201 (2003).
[15] U. Welp, V. K. Vlasko-Vlasov, X. Liu, J. K. Furdyna, and T. Wojtowicz, Phys. Rev. Lett. **90**, 167206 (2003).
[16] X. Liu, Y. Sasaki, and J. K. Furdyna, Phys. Rev. B **67**, 205204 (2003).
[17] M. Sawicki *et al.*, Phys. Rev. B **71**, 121302(R) (2005).
[18] D. Chiba, Y. Sato, T. Kita, F. Matsukura, and H. Ohno, Phys. Rev. Lett. **93**, 216602 (2004).
[19] M. Yamanouchi, D. Chiba, F. Matsukura, and H. Ohno, Nature (London) **428**, 539 (2004).
[20] G. V. Astakhov *et al.*, Appl. Phys. Lett. **86**, 152506 (2005).
[21] H. B. Callen and E. Callen, J. Phys. Chem. Solids **27**, 1271 (1966).
[22] R. P. Campion *et al.*, J. Cryst. Growth **247**, 42 (2003).
[23] Y. B. Xu, D. J. Freeland, M. Tselepi, and J. A. C. Bland, Phys. Rev. B **62**, 1167 (2000).